Engineering Microbiology 2 (2022) 100039

Contents lists available at ScienceDirect

Engineering Microbiology

journal homepage: www.elsevier.com/locate/engmic

Review

# Isolation, biosynthesis, and biological activity of rubromycins derived from actinomycetes

Ping Lin[a], Xue Li[a], Yuchen Xin[a], Hongying Li[a], Gang Li[a,*], Hongxiang Lou[a,b,*]

[a] Department of Natural Medicinal Chemistry and Pharmacognosy, School of Pharmacy, Qingdao University, Qingdao 266071, China
[b] Department of Natural Product Chemistry, Key Laboratory of Chemical Biology of Ministry of Education, School of Pharmaceutical Sciences, Shandong University, Jinan 250012, China

ARTICLE INFO

*Keywords:*
Natural products
Rubromycins
Spiroketal
Biosynthesis
Bioactivity

ABSTRACT

Natural occurring aromatic polyketides from actinomycetes indicate a structurally and functionally diverse family of polycyclic polyphenols. Some of them are consequently suggested as lead structures for drug development. Among them, rubromycins are derived from a single C26 polyketide chain and exhibit an unusual bisbenzannulated [5,6]-spiroketal system that connects a highly oxygenated naphthazarin motif to an isocoumarin unit. This type of biosynthetically elusive polycyclic polyketides has shown promising pharmacological activities, including antimicrobial, anticancer, and enzyme inhibition activity. The unique structures, intriguing biosynthesis, and marked bioactivities of rubromycins have drawn considerable attention from several chemists and biologists. This review covers the isolation, characterization, biosynthesis, and biological studies of these structurally diverse and complex rubromycins.

## 1. Introduction

Modern small molecule drug discovery seeks to discover new chemical entities that selectively and potently modulate macromolecular targets [1]. Natural products with various pharmacophores have a proven record of tremendous success in the drug discovery pipeline [2,3]. Actinomycetes are one of the most prolific sources of structurally and functionally diverse natural products [4]. Pentangular polyphenols, such as rubromycins, xantholipins, pradimicins, fredericamycins, and benastatins [5,6], belong to a growing group of actinomycetes-derived aromatic polyketides. They typically have extended "pentangular" aromatic architectures that incorporate C24–C30 polyketide chains [5,6]. These intriguingly polycyclic and structurally complex pentangular polyphenols show numerous potent bioactivities, especially antimicrobial, anti-cancer, and enzyme inhibitory activities, making them possible drug leads [7–10]. Exploration of these small molecules would facilitate the discovery of medically critical natural products for drug discovery.

Among pentangular polyphenols, natural products of the rubromycin group feature a unique bisbenzannulated [5,6]-spiroketal system connecting a highly oxygenated naphthazarin motif to an isocoumarin unit (Fig. 1A) [11,12]. They were derived from a single C26 polyketide chain. This precursor provides rubromycins after cyclization and tailoring steps [13], and also affords other aromatic polyphenols with diverse scaffolds, such as xantholipin B [14], (±)-ABX [15], and fasamycin A [16] (Fig. 1A). The major structural differences between the mature natural products in the rubromycin family are introduced during the modification steps that are catalyzed by the prevalent oxidases (Fig. 1B) [13]. Numerous rubromycins have significant antimicrobial, anti-cancer, or enzyme inhibition properties [17,18].

The unique structures, intriguing biosynthesis, and bioactivities of rubromycin polyketides received considerable attention from researchers. Unfortunately, there are only two review articles on polycyclic aromatic rubromycins in 2007 and 2015 [11,12]. They mainly presented the synthetic progress and challenges, although this group's the isolation, biosynthesis, and/or biological activities were also mentioned. However, to the best of our knowledge, detailed isolation and identification, including the spectroscopic features of the rubromycin family, have not been reviewed. Furthermore, recent biosynthetic and pharmacological difficulties and breakthroughs for this family of natural products have not been covered in the reviews.

Thus, given the current gaps in knowledge of structurally diverse and complex rubromycins, and considering the recent advances in chemical and biological studies, an amount of work dealing with the isolation, structural identification, biosynthesis, and biological evaluation of rubromycins is obtained. Here we reviewed current knowledge of the structural features of rubromycins and how to isolate and identify them efficiently. We also hope to increase awareness that the structural di-

* Corresponding authors.
*E-mail addresses:* gang.li@qdu.edu.cn (G. Li), louhongxiang@sdu.edu.cn (H. Lou).

https://doi.org/10.1016/j.engmic.2022.100039
Received 11 May 2022; Received in revised form 28 July 2022; Accepted 30 July 2022
Available online 31 July 2022

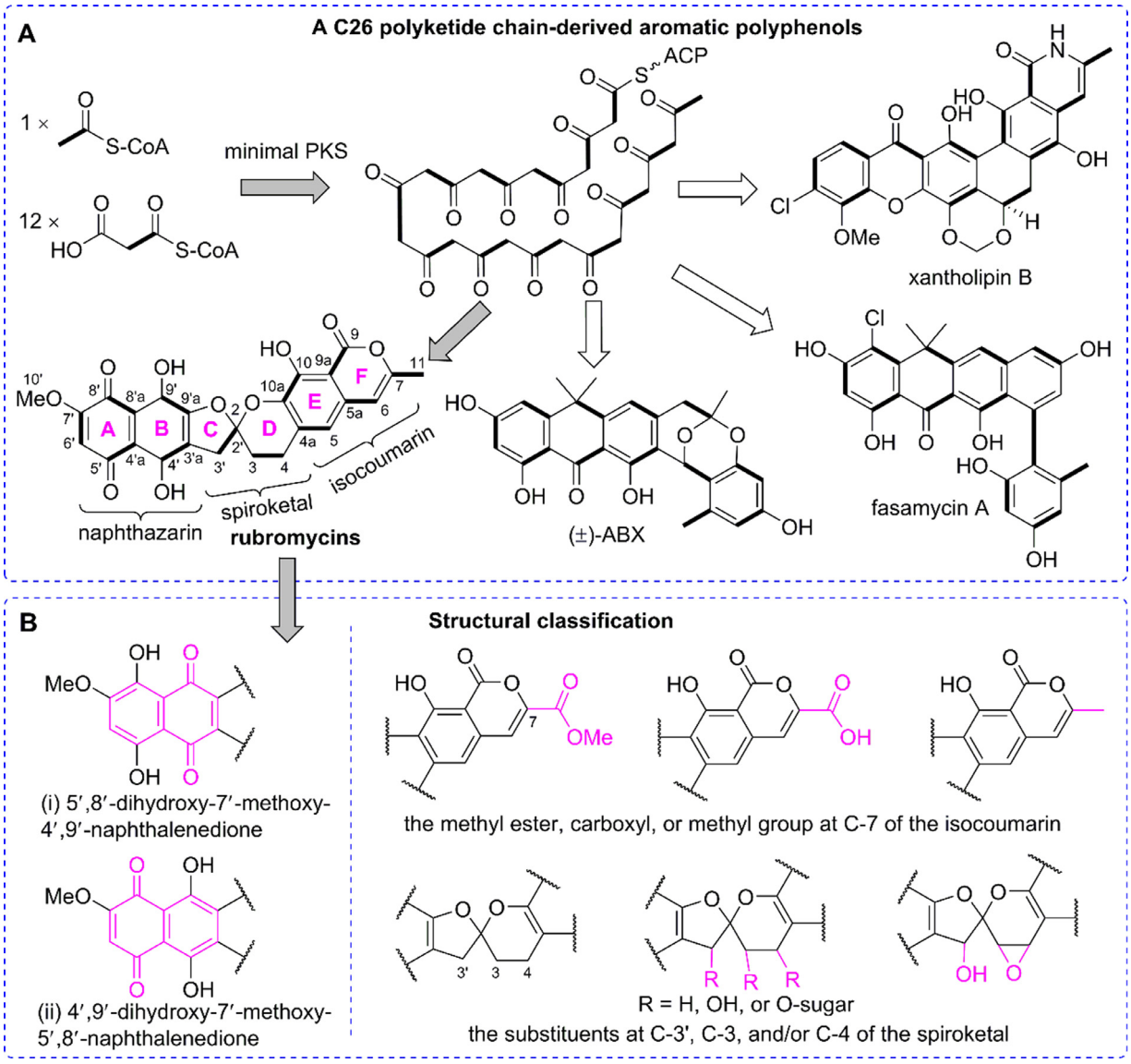


**Fig. 1.** General structure of the rubromycins. (A) Single C26 polyketide chain-derived skeletally diverse aromatic polyphenols, such as rubromycins. (B) Structural classification of rubromycins based on the oxidation and substitution characteristics. (For interpretation of the references to color in this figure, the reader is referred to the web version of this article).

versity of bioactive rubromycins mainly depends on enzymatic redox tailoring steps in the biosynthetic pathway.

## 2. Structural classification

Rubromycins belong to a large family of pentangular polyphenols that originated from a type II polyketide synthase (PKS)-derived single carbon chain in actinobacteria (Fig. 1A) [12,13]. They are generally characterized by a hexacyclic framework composed of a bisbenzannulated [5,6]-spiroketal core flanked with a highly oxygenated naphthazarin motif and an isocoumarin unit. The intriguing spiroketal formation is mediated by tailoring oxidases and disrupts the planarity of the common aromatic polyketide framework. Further tailoring proteins-induced variations in the oxidation states of the naphthoquinone ring, the carbons at C-3, C-3′, and C-4 on the spiroketal core, and the methyl group at C-7 of the isocoumarin motif [12], significantly increase the structural diversity of rubromycin derivatives, and provide the basis for structural classification. Specifically, in this review, rubromycins are firstly classified into two groups according to the oxidation states of the naphthazarin motif (Fig. 1B): (i) 5′,8′-dihydroxy-7′-methoxy-4′,9′-naphthalenediones, and (ii) 4′,9′-dihydroxy-7′-methoxy-5′,8′-naphthalenediones. The compounds are then subdivided based on the methyl ester, carboxyl, or methyl group at C-7 of the isocoumarin, followed by the substituents at C-3, C-3′, and/or C-4 of the spiroketal ring (Fig. 1B).

## 3. Chemical structures

### 3.1. Isolation

Rubromycins are isolated as amorphous red powders from actinomycetes, mainly from *Streptomyces* species (Table 1). This kind of polycyclic aromatic polyketides is often slightly soluble or even insoluble in common organic solvents, such as chloroform, methanol, dimethyl sulfoxide, and tetrahydrofuran [19,20]. This situation made them challenging to be isolated and purified; moreover, it also hindered the spectroscopic data collection for structural characterization to some extent. To address this challenge, chemical derivation by acetylation or methylation has been used as a solution for increasing solubility [19,20].

**Table 1**
Structurally diverse rubromycins or their biosynthetic precursors isolated from actinomycetes.

| Compounds | Molecular formula and weight | Source | Notable activity |
|---|---|---|---|
| $\alpha$-rubromycin (**1**) | $C_{27}H_{20}O_{12}$, 536.4450 | *S. collinus* | Antimicrobial; Anticancer; Enzyme inhibition |
| $\beta$-rubromycin (**2**) | $C_{27}H_{20}O_{12}$, 536.4450 | *S. collinus; Streptomyces* sp. A1 | Antimicrobial; Anticancer; Enzyme inhibition |
| 3′-hydroxy-$\beta$-rubromycin (**3**) | $C_{27}H_{20}O_{13}$, 552.4440 | *S. collinus* | Anticancer |
| $\beta$-rubromycin acid (**4**) | $C_{26}H_{18}O_{12}$, 522.4180 | *Streptomyces* sp. CB00271 | NR[a] |
| $\gamma$-rubromycin (**5**) | $C_{26}H_{18}O_{12}$, 522.4180 | *S. collinus* | Antimicrobial; Anticancer; Enzyme inhibition |
| $\delta$-rubromycin (**6**) | $C_{26}H_{18}O_{11}$, 506.4190 | *Streptomyces* sp. A1 | Anticancer |
| purpuromycin (**7**) | $C_{26}H_{18}O_{13}$, 538.4170 | *Actinoplanes ianthinogenes* | Antimicrobial; Anticancer |
| heliquinomycin (**8**) | $C_{33}H_{30}O_{17}$, 698.5860 | *Streptomyces* sp. MJ929-SF2 | Antimicrobial; Anticancer; Enzyme inhibition |
| 9′-methoxy-heliquinomycin (**9**) | $C_{34}H_{32}O_{17}$, 712.6130 | *S. piniterrae* sp. nov. | NR[a] |
| DK-7814-A (**10**) | $C_{26}H_{18}O_{15}$, 570.4150 | *Dactylosporangium* sp. | NR[a] |
| DK-7814-B (**11**) | $C_{26}H_{18}O_{14}$, 554.4160 | *Dactylosporangium* sp. | NR[a] |
| DK-7814-C (**12**) | $C_{26}H_{16}O_{14}$, 552.4000 | *Dactylosporangium* sp. | NR[a] |
| rubromycin CA1 (**13**) | $C_{25}H_{16}O_{12}$, 508.3910 | *S. hyaluromycini* MB-PO13 | Antimicrobial |
| rubromycin CA2 (**14**) | $C_{25}H_{16}O_{13}$, 524.3900 | *S. hyaluromycini* MB-PO13 | Antimicrobial |
| hyaluromycin (**15**) | $C_{30}H_{21}NO_{13}$, 603.4920 | *S. hyaluromycini* MB-PO13 | Enzyme inhibition |
| griseorhodin A (**16**) | $C_{25}H_{16}O_{12}$, 508.3910 | *S. californicus* JA 2640 | Antimicrobial; Anticancer |
| griseorhodin C (**17**) | $C_{25}H_{18}O_{13}$, 526.4060 | *S. californicus* JA 2640 | Anticancer |
| griseorhodin G (**18**) | $C_{25}H_{18}O_{12}$, 510.4070 | *S. griseus* FCRC-57 | NR[a] |
| 3,4-dideoxygriseorhodin C (**19**) | $C_{25}H_{18}O_{11}$, 494.4080 | *Streptomyces* sp. No.76 | Antimicrobial |
| 4-methoxygriseorhodin C (**20**) | $C_{26}H_{20}O_{13}$, 540.4330 | *Streptomyces* sp. SIPI-$A_5$-0044 | Antimicrobial |
| 3,4-dideoxy-3′-oxo-griseorhodin C (**21**) | $C_{25}H_{16}O_{11}$, 492.3920 | *A. ianthinogenes* ATCC 20884 | NR[a] |
| collinone (**22**) | $C_{27}H_{18}O_{12}$, 534.4290 | Heterologous host *S. coelicolor* CH999 (*rub* gene cluster from *S. collinus* DSM2012) | Antimicrobial |
| dihydrocollinone (**23**) | $C_{27}H_{20}O_{12}$, 536.4450 | Heterologous host *S. albus* J1074 (*grh* gene cluster from *Streptomyces* sp. JP95) | NR[a] |
| secocollinone (**24**) | $C_{27}H_{20}O_{13}$, 552.4440 | Same to the above strain | NR[a] |
| (**25**) | $C_{27}H_{20}O_{14}$, 568.4430 | Same to the above strain | NR[a] |
| lenticulone (**26**) | $C_{26}H_{16}O_{12}$, 520.4020 | Same to the above strain | Antimicrobial |
| dihydrolenticulone (**27**) | $C_{26}H_{18}O_{12}$, 522.4180 | Same to the above strain | NR[a] |
| shunt product (**28**) | $C_{26}H_{18}O_{12}$, 522.4180 | Same to the above strain | NR[a] |

[a] NR: not recorded in this table due to the weak activity or no reported biological activity.

#### 3.1.1. 5′,8′-dihydroxy-7′-methoxy-4′,9′-naphthalenediones

Rubromycin family starts with $\alpha$-rubromycin (**1**, previously called collinomycin [21,22]) and $\beta$-rubromycin (**2**, previously called rubromycin [22,23]) with vivid red color (Fig. 2). Both were isolated from a culture broth of *Streptomyces collinus* by Brockmann and Renneberg in 1953 [21,23]. Among them, compound **1** is the only exceptional rubromycin member in which the spiroketal ring is open. Notably, until 2000, the correct planar structure of compound **2** was determined by Zeeck and co-workers based on the NMR data and an isotope labeling experiment on a rubromycin-producing strain *Streptomyces* sp. A1 [20]. During these chemical investigations, one additional $\beta$-rubromycin derivative, 3′-hydroxy-$\beta$-rubromycin (**3**, Fig. 2), was isolated and identified [20]. The only chiral center at C-2 that occurred in the spiroketal of the above rubromycins was successfully assigned as *S*-configured based on the electronic circular dichroism (ECD) spectra and quantum chemical calculations in the year 2000 [24].

Recently, Zhu and co-workers focused on the genome mining of the rubromycin natural products using a putative spiroketal formation-specific monooxygenase RubN as the probe [25]. Fifty-four potential rubromycins-related biosynthetic gene clusters (BGCs) were found based on National Center for Biotechnology Information (NCBI) database and antibiotics & Secondary Metabolite Analysis Shell (antiSMASH) analysis, and one was found to be derived from *Streptomyces* sp. CB00271 which was stored in the researchers' lab. Further chemical examination of this strain indicated the high yield of compound **2** (more than 120 mg/L) and afforded a new congener $\beta$-rubromycin acid (**4**, Fig. 2) with a carboxyl group at C-7 [25].

#### 3.1.2. 4′,9′-dihydroxy-7′-methoxy-5′,8′-naphthalenediones

Chemical investigations undertaken by the Zeeck group in 1966 showed a red pigment, $\gamma$-rubromycin (**5**, Fig. 3) from *S. collinus* [22]. They also reported the isolation and identification of $\delta$-rubromycin (**6**, Fig. 3) from the rubromycin-producing strain, *Streptomyces* sp. A1 [20]. Purpuromycin (**7**, Fig. 3) as bright purple crystals was derived in 1974 from the culture broth of *Actinoplanes ianthinogenes* isolated from a soil sample in Blumenau, Brazil [26]. The planar structure of compound **7** was determined using spectroscopic data and chemical degradations [27]. Its relative configuration was tentatively assigned through the studies on the stereochemistry of the bisphenolic spiroketal unit [28]. In 1996, another soil-derived *Streptomyces* sp. MJ929-SF2 obtained in Tokyo, Japan, yielded a red rubromycin, heliquinomycin (**8**, Fig. 3), with a unique L-cymarose moiety C-3′ [29]. Its stereochemistry, including an R-configured spiro center, was established through the X-ray diffraction data and the sugar analysis after compound **8** acid hydrolysis [30]. Note that its spiro center exhibited an *R* absolute configuration opposite to metabolites **2–7** [24]. In 2019, a new 9′-methoxy derivative of heliquinomycin (**9**, Fig. 3), and compound **8** were uncovered by Huang and co-workers from the culture broth of a new *Streptomyces* species, *S. piniterrae* sp. nov. [31,32]. The DK-7814-A, B, and C (**10–12**, Fig. 3) were isolated from the bacterium *Dactylosporangium* sp. [12]. Compared with other members of the rubromycin family, they were highly oxygenated at the spiroketal moiety.

Harunari et al. reported the discovery of three rubromycin derivatives, rubromycins CA1 and CA2 (**13** and **14**, Fig. 4) and hyaluromycin (**15**, Fig. 4), from *S. hyaluromycini* MB-PO13 that was chosen from about

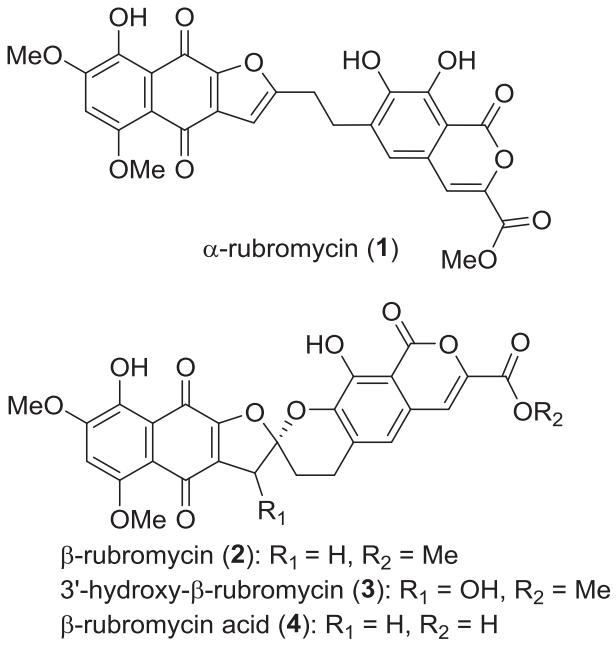


**Fig. 2.** Chemical structures of compounds **1–4** with a 5′,8′-dihydroxy-7′-methoxy-4′,9′-naphthalenedione.

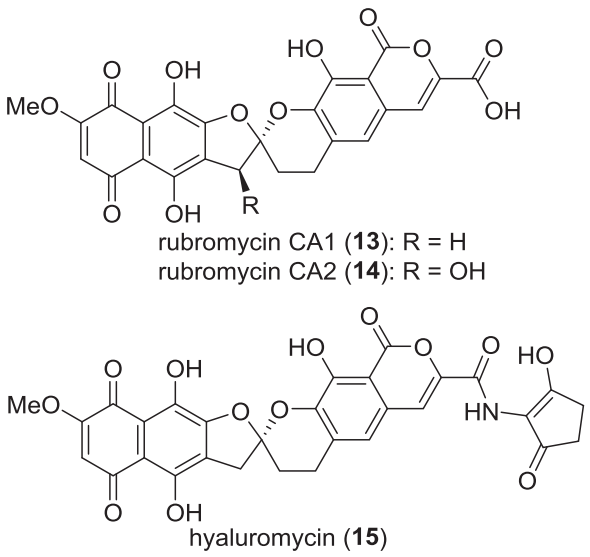


**Fig. 4.** Chemical structures of compounds **13–15**.

1000 marine actinomycetes [33,34]. Compared with the co-occurring compounds **13** and **14** containing a carboxylated isocoumarin, compound **15** possessed an amide substituent of the isocoumarin unit using a unique 2-amino-3-hydroxycyclopent-2-enone moiety [33].

The griseorhodins (**16–21**, Fig. 5) belong to a unique subgroup of the rubromycin family containing a methyl group at C-7. Similar to compounds **8–12**, they were also highly oxygenated at the spiroketal moiety. Griseorhodin A (**16**) was isolated in 1961 from the antibacterial extract of *S. californicus* JA 2640 for the first time [35,36], and its planar structure with a unique epoxide ring between C-3 and C-4 became clear in 1978 based on the Mass Spectrometry (MS) and Nuclear Magnetic Resonance (NMR) data, together with chemical reactions [37]. During these chemical and structural studies, another member of the griseorhodins, griseorhodin C (**17**), was also discovered [38]. Compounds **16** and **17** had their absolute configurations as *2S,3S,4S,3′S* [39] and *2S,3S,4R,3′R* [40,41], respectively, which was supported by the theoretical calculations of ECD and/or vibrational circular dichroism.

In 1979, antimicrobial and cytotoxic culture broth from *S. griseus* FCRC-57 isolated from a crop soil at Mayland, U.S.A., yielded griseorhodin G (**18**, Fig. 5), in addition to structurally related compounds **16** and **17** [42]. Further chemical investigations on different actinomycete strains *Streptomyces* sp. No.76, *Streptomyces* sp. SIPI-$A_5$-0044, and *A. ianthinogenes* ATCC 20884 led to the isolation and characterization of 3,4-dideoxygriseorhodin C (**19**, also called 7,8-dideoxygriseorhodin C) [43], 4-methoxygriseorhodin C (**20**, also called 8-methoxygriseorhodin C) [44], and 3,4-dideoxy-3′-oxo-griseorhodin C (**21**, also called 7,8-dideoxy-6-oxo-griseorhodin C) (Fig. 5) [19], respectively. In 2020, the absolute configuration of compound **19** was found to be *2S,3′S* using the ROESY spectroscopic data and comparing the measured and calculated ECD spectra [45].

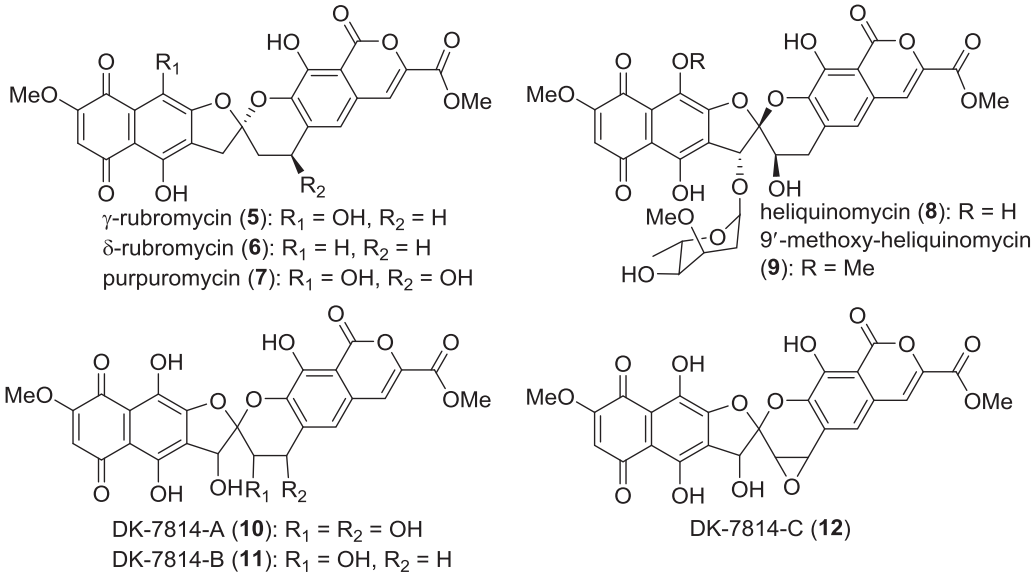


**Fig. 3.** Chemical structures of compounds **5–12**.

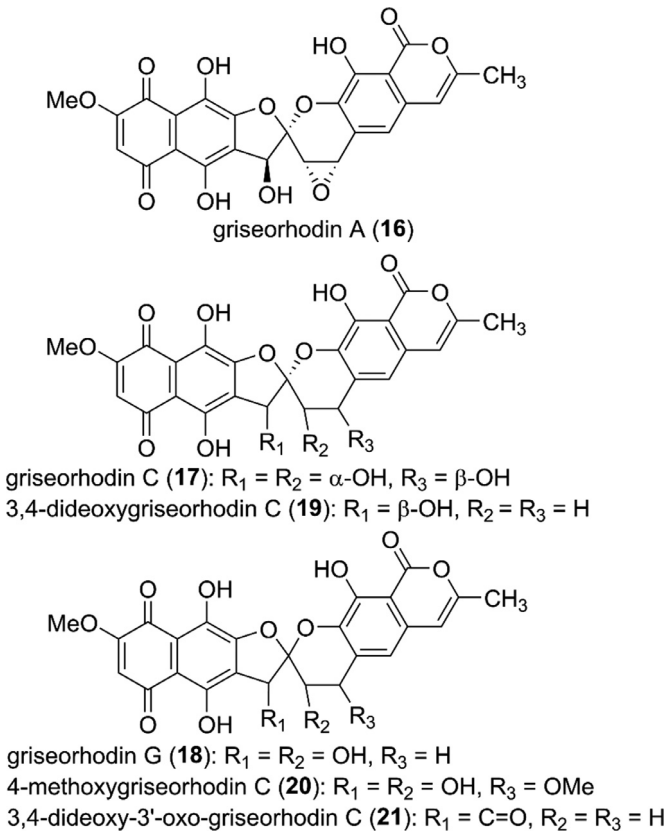


**Fig. 5.** Chemical structures of compounds **16**–**21**.

### 3.2. Spectroscopic characteristics for identification

The low solubility of rubromycins in organic solvents greatly influences the quality and readability of spectroscopic data [19,20]. By documenting using the above references, the $^{1}$H and $^{13}$C NMR spectra in the solvent DMSO-$d_6$ are the frequently used data for elucidating the structure of rubromycin-type pigments. Their $^{1}$H NMR spectra could be fastest measured in a few minutes and provide critical information on many aromatic/olefinic protons and oxygenated methines and also exchangeable protons [46], while their $^{13}$C NMR spectra indicated some aromatic, olefinic, or carbonyl carbons, in addition to a few saturated carbon signals.

Generally, the $^{1}$H NMR spectra of rubromycins in the solvent DMSO-$d_6$ showed the existence of three exchangeable protons related to 10-OH, 9′-OH, and 4′-OH (Fig. 6A) [25,34,40]. Their chemical shifts are around 11.0, 12.0, and 13.0 ppm, respectively. Conversely, compounds **1**–**4** with a methoxy group at C-5′ on the naphthazarin unit only display two hydroxyl group signals at about 11.0 and 13.0 ppm. The proton signals of aromatic/olefinic H-5, H-6, and H-6′ ranging from 6.0 to 8.0 ppm are observed as singlets (Fig. 6A). The highly oxygenated spiroketal ring was shown by the occurrence of oxygenated methines and corresponding hydroxyl groups that are located in the range of chemical shift values from 4.0 to 6.5 ppm (Fig. 6B). It has to mention the frequently observed splitting signals H-3′ and 3-OH and their coupling constant (around 7.5 Hz in compound **14**) that are useful for determining the oxidation state of spiroketal (Fig. 6C) [34]. Additionally, the methoxy group at C-7′ with the chemical shift value of around 3.8 ppm is an important signal for rubromycins. Other distinguishable structural characteristics in the $^{1}$H NMR spectrum, such as the C-7 methyl (around 2.2 ppm), are also crucial for determining the structures of some rubromycins.

Nevertheless, suppose rubromycins have substantial amounts and are soluble in deuterated solvents for further NMR measurements. In that case, the $^{13}$C NMR spectrum is a vital addition to aid in verifying the known structures of rubromycins or analyzing the structural features of the new derivatives [25,34]. Two $\alpha,\beta$-unsaturated carbonyl carbons should be found in the low-field region of the $^{13}$C NMR spectrum and show chemical shift values of about 180 ppm (Fig. 6C). Typically, most rubromycins possess nine carbon signals ranging from 140 to 170 ppm, which are related to the oxygenated aromatic/olefinic carbons and the carboxyl or ester groups. Nine aromatic/olefinic carbons and one carbon corresponding to the ketal group are observed in the chemical shift range from 100 to 140 ppm (Fig. 6C) [25,34]. The chemical shift values of three saturated carbons at C-3, C-3′, and C-4 are less than 40.0 ppm. They could move to the downfield region of the $^{13}$C NMR spectrum if the corresponding carbons are oxygenated. The remaining carbon signals at $\delta_C$ 51.0–57.0 ppm are generally from the methoxy groups. It can be stated that more two-dimensional NMR data are needed to fully elucidate the structures of novel rubromycin members [31].

Currently, the single crystal X-ray diffraction technique is a powerful tool for rubromycin structural elucidation, such as the absolute configuration of compound **8** [30]. The circular dichroism (CD) spectrum and its theoretical chemical calculations are also widely accepted approaches for studying the chemical structures of rubromycins. The absolute stereochemistry of the spiro center at C-2 (or C-2′) in most rubromycins, such as rubromycins **2** [24], **5** [24], **15** [33], **16** [39], and **19** [45], was assigned as *S* based on the characteristic CD cotton effects, including a positive one at around 220 nm and a negative one at around 260 nm. The only exception, an *R* configuration of the spiro center, comes from compound **8** [29,30].

## 4. Biosynthesis

### 4.1. Rubromycin BGCs

Developing microbial genomics and omics-related technology helps to understand the BGCs of rubromycins [1]. A single C26 polyacetate chain was initially constructed by a minimal PKS that contains a ketosynthase $\alpha$ ($KS_\alpha$), a ketosynthase $\beta$/chain-length factor ($KS_\beta$/CLF), and an acyl carrier protein (ACP) [13]. Further cyclization and aromatization of the PKS-derived polyketide chain followed by tailoring processes afford diverse rubromycins [13]. The above-mentioned biosynthetic origin could be partially supported by feeding $^{13}$C-labeling acetate, malonic acid, methionine, or glucose to the rubromycin-producing bacterial strains (Fig. 7), such as *Streptomyces* sp. A1 that yielded $\beta$-rubromycin (**2**) [20] and *Streptomyces* sp. MJ929-SF2 that afforded heliquinomycin (**8**) [47].

In 2001, the introduction of the putative rubromycin BGC (*rub*)-containing chromosomal DNA fragments of *S. collinus* DSM2012 into a heterologous host *S. coelicolor* CH999 resulted in many transformants [48]. One of them, MRB6C, produced a red angular hexacyclic tridecaketide, collinone (**22**), which did not have a spiroketal core and may serve as an intermediate for further spiroketalization [48]. Shortly after, Li and Piel firstly cloned, fully sequenced, and unambiguously identified the griseorhodin A (**16**) BGC (*grh*) from a marine-derived *Streptomyces* sp. JP95 through heterologous expression and knock-out experiments [5,49]. This BGC spans a 34.2 kb region and comprises 33 open reading frames (ORFs) [49]. Intriguingly, 11 ORFs encoding different oxidoreductases were discovered and proposed to be responsible for the post-PKS modifications of the hexacyclic precursor-like compound **22** [5], which was accompanied by the formation of the highly oxygenated spiroketal ring system [49].

### 4.2. Key enzymes for yielding [5,6]-spiroketal

To identify the oxidoreductases responsible for spiroketal formation, the Piel group constructed 14 gene-deletion variants of the gene cluster *grh* isolated from *Streptomyces* sp. JP95 in 2009 [39]. Each gene cluster was then heterologously expressed in *S. albus* J1074 to

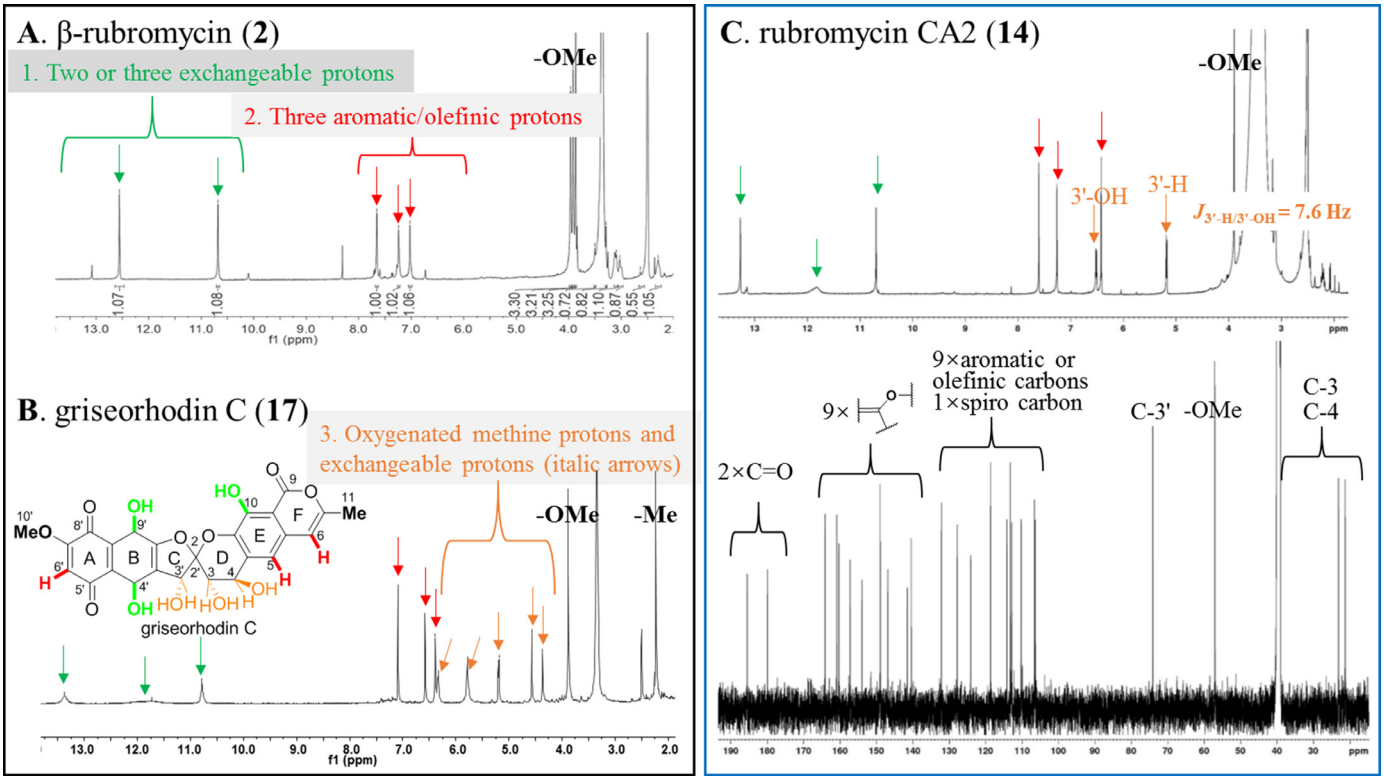


**Fig. 6.** Spectroscopic features of rubromycins. Colored arrows and brackets indicate the key diagnostic information in (A) the $^{1}$H NMR spectrum of *β*-rubromycin (**2**) [25], (B) the $^{1}$H NMR spectrum of griseorhodin C (**17**) [40], and (C) the $^{1}$H and $^{13}$C NMR spectra of rubromycin CA2 (**14**) (Adapted with permission from [34]. Copyright 2022 American Chemical Society).

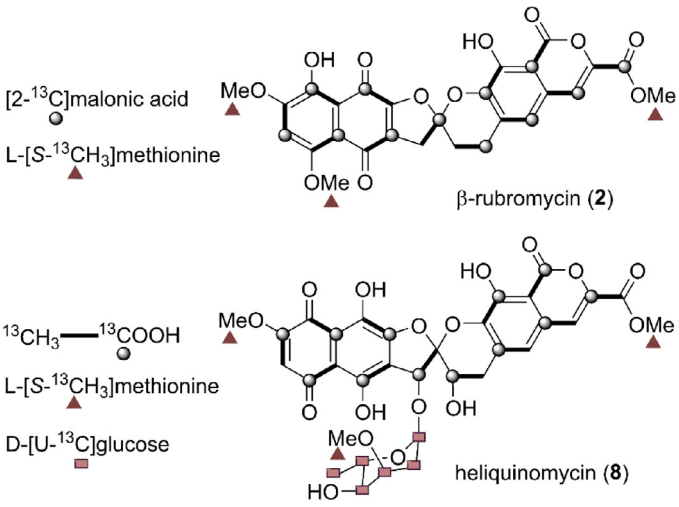


**Fig. 7.** Biosynthetic origins of carbons in *β*-rubromycin (**2**) and heliquinomycin (**8**) based on isotope labeling experiments (For interpretation of the references to color in this figure, the reader is referred to the web version of this article).

produce rubromycin intermediates. Further chemical investigation of the engineered strains afforded the final product **16**, and allowed the isolation and identification of some key intermediates, including 3,4-dideoxygriseorhodin C (**19**), **22**, and lenticulone (**26**) (Fig. 8) [39], supporting the fact that the spiroketal core is constructed by breaking four carbon-carbon bonds in **22**. Compound **26**, as a novel rubromycin derivative with a unique [6,6]-spiroketal moiety, was obtained from the *grhO6* mutant of the strain JP95, showing a possible role of GrhO6 in promoting carbon-carbon bond cleavage [39]. Recently, Frensch et al. constructed key enzymatic redox tailoring steps of the biosynthesis of rubromycins *in vitro* and elucidated the structures of reactive intermediates, verifying that four carbon-carbon bonds were broken and two $CO_2$ molecules were removed in the biosynthetic pathway of rubromycin-type polyketides (Fig. 8) [13]. During these enzymatic reactions, a multifunctional flavoprotein monooxygenase GrhO5 was found to primarily initiate and mediate spiroketal formation [13]. The GrhO5 and its functional homolog RubL from rubromycin biosynthesis have recently been analyzed mechanistically and structurally [13,50]. They featured a W fingerprint motif and were suggested to belong to a new subgroup of group A flavoprotein monooxygenases (FPMOs) with three domains in which domains I and II are responsible for flavin adenine dinucleotide (FAD) and substrate binding, respectively [50]. The intriguing W residue was proposed to allow key aromatic sandwich $\pi$-$\pi$ stacking interactions with the FAD cofactor and play a dual role in the tethering and shielding of FAD [50].

Altogether, a highly reactive ACP-binding polyketone chain was firstly generated by the minimal PKS that used an acetyl-CoA starter and 12 malonyl-CoA extender units (Fig. 8). Further regioselective ketoreduction at C-19 [5], cyclization, aromation, and tailoring processes afforded a highly oxidized precursor, collinone (**22**). The flavoprotein monooxygenase GrhO5 further activated the ring A reduction of **22** into dihydrocollinone (**23**) [50]. Compound **23** was further modified using GrhO5 through an aromatic hydroxylation reaction to form the unstable intermediate secocollinone (**24**), whose structure was determined by chemical derivation with methylation [13]. Compound **24** was then transformed into **25**, which may automatically undergo the third carbon-carbon bond cleavage through facile decarboxylation/oxidation, promoting the formation of lenticulone (**26**) and dihydrolenticulone (**27**) with a [6,6]-spiroketal, together with the shunt product **28** (Fig. 8) [13,50]. It should be noted that the formation of the shunt product was inhibited by the flavoprotein oxidase GrhO1, which probably boosted the production of **27** through the oxidation of ring B in **25** [13]. Finally, another flavoprotein, monooxygenase GrhO6, enabled the sub-

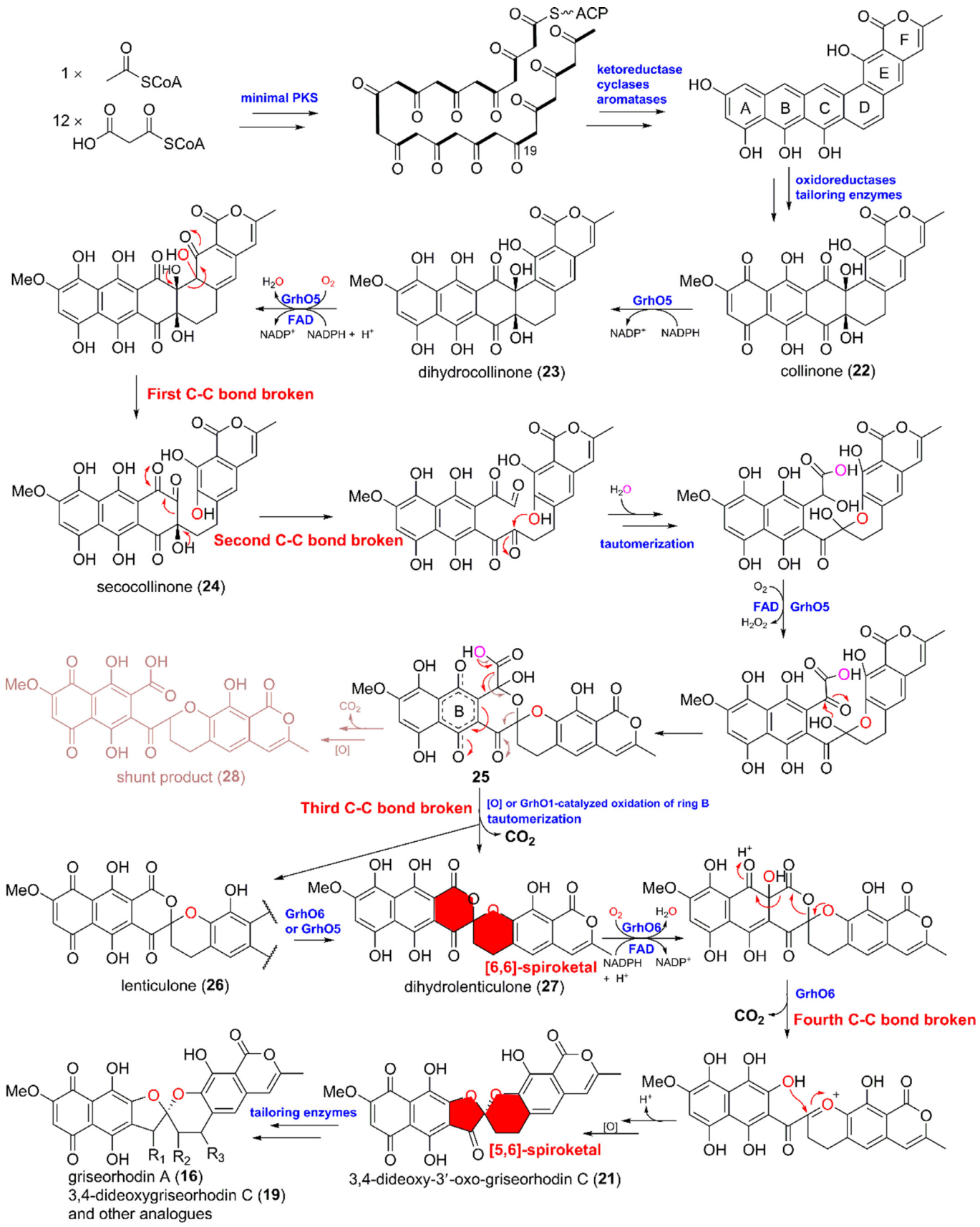


**Fig. 8.** The proposed enzymatic [5,6]-spiroketal formation in the rubromycin biosynthetic pathway. Two flavoprotein monooxygenases GrhO5 and GrhO6, and the flavoprotein oxidase GrhO1 were involved in the spiroketal formation reactions, during which four carbon-carbon (C-C) bonds were broken and two carbon dioxide ($CO_2$) molecules were removed. The structures of numbered compounds **21**–**28** were determined by NMR, LC-HRMS, and/or chemical derivations.

sequent decarboxylation through the fourth carbon-carbon bond cleavage, which completed the formation of the [5,6]-spiroketal ring system seen in mature rubromycin polyketides [13]. Various tailoring enzymes, such as the glycosyltransferase in the BGC of compound **8** [32], introduced several structural features presented in rubromycin-class compounds (Figs. 7 and 8). It should be mentioned here that the dimeric forms could be the precursors of the post-PKS steps [51], which was proposed because of the presence of dimeric griseorhodins D1 and D2 in the *grhM* mutant of *Streptomyces* sp. JP95 and the *Streptomyces* sp. CN48+ [39,51].

## 5. Biological activity

### 5.1. Antimicrobial activity

Rubromycins have attracted much attention due to their antimicrobial activity [20,42]. Compared with rubromycins **1** and **2**, $\gamma$-rubromycin (**5**) exhibited a significantly stronger antibacterial activity against Gram-positive *Staphylococcus aureus* ATCC 6538, *Micrococcus luteus* ATCC 15307, and *Bacillus subtilis* ATCC 6633 with MIC values ranging from 0.01 to 0.08 $\mu$g/mL, and had a more intriguing antifungal activity against *Saccharomyces cerevisiae* ATCC 204508 (MIC = 1.6 $\mu$g/mL) [18]. These results showed that the naphthazarin featured in compound **5** should be essential for antimicrobial activity. Additionally, it seems that the [5,6]-spiroketal is not crucial for activity due to the relatively close MIC values of **1** and **2**.

Purpuromycin (**7**), with similar structural features as that of **5**, also showed strong antibacterial efficiencies against Gram-positive *Staphylococcus* and *Streptococcus* species at the concentrations of 0.03–0.06 $\mu$g/mL [19,26]. It also had moderate inhibitory activity against the Gram-negative bacteria *Escherichia coli* SKF 12140 and *Proteus vulgaris* X19H with MIC values of around 4.0 $\mu$g/mL, and the fungal pathogen *Candida albicans* SKF 2270 with an MIC value of 0.25 $\mu$g/mL [19,26]. Compared with **7**, compound **21** exhibited a significantly weaker anti-Gram-positive bacterial activity, and even no activity against Gram-negative bacteria and *C. albicans* [19]. It is also notable that compounds **19** and **20** showed a selective inhibitory effect on Gram-positive bacteria, including methicillin-resistant *S. aureus* (MRSA; MIC values less than 0.8 $\mu$g/mL) [44,45]. Intriguingly, compound **19** also synergized with the $\beta$-lactam antibiotic oxacillin against MRSA, resulting in an approximately tenfold reduction in the MIC value [45]. The above results proposed that the oxidation at C-3′ and/or the methyl at C-7 should be responsible for the inactive or reduced activity against Gram-negative bacteria and fungi.

As expected, heliquinomycin (**8**), as a 3′-O-glycoside, was inactive against Gram-negative bacteria and fungi, while it showed promising pharmacological activity against several MRSA strains with MIC values of less than 0.1 $\mu$g/mL [29]. Additionally, compound **13** with a free $CH_2$-3′ was a more biologically potent polyketide compared with compound **14** with an oxygenated C-3′. It showed a MIC value of 0.2 $\mu$g/mL against *S. aureus* IFO 12732 and a MIC value of 6.3 $\mu$g/mL against *C. albicans* NBRC 1594 [34]. These works further supported the negative influence of the C-3′ oxidation on antimicrobial activity. It should be noted that the reduced antimicrobial activity was also likely related to the [6,6]-spiroketal or the oxidation at C-3 and C-4, which was suggested through an antibacterial assay for compounds **16, 19**, and **26** [39].

### 5.2. Anticancer property

Several rubromycins were reported to have cytotoxic properties. Rubromycins **2, 3, 5**, and **6** possessed comparable cytotoxic activity against MCF-7, HMO2, Kato III, and HEP G2 cancer cell lines compared with the positive drug doxorubicin [20]. It was also reported that compounds **1, 2**, and **5** had little or no cytotoxicity against cancer cell lines A549 and PC3 [18]. Compound **8** showed quite similar biological activity against many tumor cell lines HeLa S3, Leukemia L1210, Carcinoma IMC, Melanoma B16, and Fibrosarcoma FS-3 with $IC_{50}$ values of 1.6, 0.97, 1.56, 0.89, and 0.83 $\mu$g/mL, respectively [29]. Other compounds, such as griseorhodins, had moderate cytotoxicity at micromolar concentrations [39,42].

Telomerase, as a ribonucleoprotein complex elongating telomeric DNA, is vital for the immortality of cancer cells and has become an intriguing target for cancer treatment [52,53]. Among them, compounds **2** and **5** significantly inhibited human telomerase with $IC_{50}$ values of around 3 $\mu$M [54]. It is notable that the opening of the spiroketal system in compound **1** substantially diminished its activity toward human telomerase ($IC_{50}$ > 200 $\mu$M) [54], highlighting that the spiroketal plays a pivotal role in telomerase inhibition. This theory was also verified by biosynthetically related spiroketal-containing compounds **7, 16**, and **17** that displayed comparable anti-telomerase activity as **2** and **5**. Yuen et al. chemically synthesized and biologically evaluated **5** and **29** modified spiroketal analogs, and concluded that the isocoumarin subunit is also crucial in telomerase inhibition [17]. Therefore, rubromycins with the intact [5,6]-spiroketal and isocoumarin units are potent inhibitors of human telomerase.

### 5.3. Enzyme inhibition

Initially, rubromycins were recognized as inhibitors of human immunodeficiency virus-1 (HIV-1) reverse transcriptase (RT) because compounds **2** and **5** provided RT inhibition constant (Ki) values of 0.27 and 0.13 $\mu$M, respectively [20,55]. The inhibition of DNA helicase was also noticed in rubromycin-type compounds, as supported by molecule **8** at concentrations between 5 and 10 $\mu$g/mL in a non-competitive manner with a Ki value of 6.8 mM [29]. Interestingly, compound **15** had 25-fold more potent inhibition toward hyaluronidase than well-known inhibitor glycyrrhizin, while **2** and **5** exhibited no inhibitory activity [33]. These results showed that the $C_5N$ substituent in **15** is crucial for inhibiting hyaluronidase.

In 2000, Mizushina et al. reported that rubromycins **1** and **2** selectively inhibited animal DNA polymerases but not prokaryotic and plant DNA polymerases. Additionally, compound **1** was found not to be an inhibitor of HIV-1 RT, enabling the authors to classify rubromycins as selective inhibitors of the animal polymerases rather than HIV RT inhibitors [56]. Particularly intriguing are the dose-dependent inhibitory effects on polymerase $\beta$. Specifically, compound **1** strongly inhibited the polymerase $\beta$ activity with a Ki value of 0.17 $\mu$M through binding to the active region competing with the nucleotide substrate, while the Ki value for **2** is 10.5 $\mu$M [56].

Recently, a bioassay-guided chemical investigation on *S. collinus* ATCC19743 afforded compound **1** as a potential anti-SARS CoV-2 agent targeting the main protease ($M^{pro}$) ($IC_{50}$ = 5.4 ± 0.2 $\mu$M) [57]. Considering its significant cytotoxic activity against normal human fibroblasts ($CC_{50}$ = 16.7 $\mu$M) and poor drug-like properties, Rateb and co-workers applied many artificial intelligence-guided tools to optimize **1**, providing a more appropriate aromatic scaffold [57]. A pharmacophore-based similarity search finally followed this in FDA-approved medications to provide cromoglicic acid with more antiviral potential than **1**. The above results provide an impetus for assigning the rubromycin scaffold without the [5,6]-spiroketal unit as a template for modification to obtain more potent and selective enzyme inhibitors.

Other reported activities may also be related to enzyme regulation. For example, by applying axolotl embryo tail regeneration assay, **5** at 1 $\mu$M was first recognized as an inhibitor of tail regeneration, although the underlying mechanism remains unclear [18]. Recently, compound **2** inhibited cyst germination in *Phytophthora infestans*, possibly because of the up-regulation of an RIO kinase-like gene PITG_04584 [58].

## 6. Conclusions and future perspectives

Natural products are invaluable sources of inspiration for chemistry and biology [59]. The naturally occurring rubromycins with vivid red

colors have gathered considerable attention because of their highly oxygenated and complex structures with obvious biological activities. Their isolation, structural elucidation, biosynthesis, and biological activity are increasingly being described in recent decades. Here, we present a comprehensive review of rubromycins from actinobacteria, especially *Streptomyces* species, together with some confirmed or proposed biosynthetic precursors. Their most intriguing structural feature is the bisbenzannulated [5,6]-spiroketal system, which results from the elusive catalyzing capability of prevalent tailoring oxidases in the biosynthetic pathway of rubromycins. Additionally, this class of secondary metabolites displays marked biological functions, such as antimicrobial, anticancer, and enzyme inhibitory activities.

Although recent decades have seen noticeable successes in chemical studies on this group of pentangular polyphenols, their isolation and structural elucidation are challenging in terms of their soluble or insoluble properties in common organic solvents. This might be why no more than 30 members have been identified since the first isolation in 1953 (Table 1). Perhaps, liquid chromatography's high-resolution mass spectrometry is an appropriate method for quickly screening and tentatively identifying them without isolation and purification [60,61]. Chemical derivation by acetylation or methylation is a good solution for increasing solubility, followed by isolation for structural characterization. Nevertheless, the $^{1}$H NMR spectrum, as the fastest measured NMR data, is strongly suggested as it provides rich diagnostic data related to structural and configurational information of rubromycins.

The development of microbial genomics and omics-related technology with the help of artificial intelligence tools facilitates the understanding of the rubromycins biosynthetic pathway [1]. Currently, three key redox enzymes have been assessed *in vitro* and are responsible for the [5,6]-spiroketal formation through a [6,6]-spiroketal ring system. However, many tailoring and regulatory genes encoding proteins responsible for rubromycin scaffold modifications, such as hydroxylations at C-3 and/or C-4, remain unclear. It is expected that the current progress paves the way for the future enzymatic generation of more rubromycin analogs, especially those with new molecule scaffolds.

It is convincing that the naphthazarin moiety and the free methylene at C-3′ are critical for antimicrobial activity, exemplified by the most bioactive compound $\gamma$-rubromycin (**5**). In contrast, rubromycins with the intact [5,6]-spiroketal and isocoumarin units are strong inhibitors of human telomerase, making them potent drug leads for cancer treatment. Rubromycins are also clarified as selective enzyme inhibitors, especially for animal polymerases. However, the structure-activity relationship (SAR) of rubromycins, especially activity related to quinone, spiroketal, and isocoumarin units remains elusive. The complex structures and diverse bioactivity of the rubromycin molecules have aroused research interest in chemical and biological communities, and clear SAR could be expected in the future.

## Declaration of Competing Interest

The authors declare that they have no known competing financial interests or personal relationships that could have appeared to influence the work reported in this paper.

## Acknowledgments

This work was financially supported by the National Natural Science Foundation of China (No. 81903494) and the Scientific Research Foundation of Qingdao University.

## References

[1] G. Li, P. Lin, K. Wang, et al., Artificial intelligence-guided discovery of anticancer lead compounds from plants and associated microorganisms, Trends Cancer 8 (1) (2022) 65–80, doi:10.1016/j.trecan.2021.10.002.
[2] D.J. Newman, G.M. Cragg, Natural products as sources of new drugs over the nearly four decades from 01/1981 to 09/2019, J. Nat. Prod. 83 (3) (2020) 770–803, doi:10.1021/acs.jnatprod.9b01285.
[3] A.G. Atanasov, S.B. Zotchev, V.M. Dirsch, et al., Natural products in drug discovery: advances and opportunities, Nat. Rev. Drug. Discov. 20 (3) (2021) 200–216, doi:10.1038/s41573-020-00114-z.
[4] P.A. Jose, A. Maharshi, B. Jha, Actinobacteria in natural products research: progress and prospects, Microbiol. Res. 246 (2021) 126708–126721, doi:10.1016/j.micres.2021.126708.
[5] G. Lackner, A. Schenk, Z. Xu, et al., Biosynthesis of pentangular polyphenols: deductions from the benastatin and griseorhodin pathways, J. Am. Chem. Soc. 129 (30) (2007) 9306–9312, doi:10.1021/ja0718624.
[6] Y. Chen, E. Wendt-Pienkoski, S.R. Rajski, et al., *In vivo* investigation of the roles of FdmM and FdmM1 in fredericamycin biosynthesis unveiling a new family of oxygenases, J. Biol. Chem. 284 (37) (2009) 24735–24743, doi:10.1074/jbc.M109.014191.
[7] L.C. Almeida, A. Bauermeister, P. Rezende-Teixeira, et al., Pradimicin-IRD exhibits antineoplastic effects by inducing DNA damage in colon cancer cells, Biochem. Pharmacol. 168 (2019) 38–47, doi:10.1016/j.bcp.2019.06.016.
[8] W. She, W. Ye, A. Cheng, et al., Discovery, bioactivity evaluation, biosynthetic gene cluster identification, and heterologous expression of novel albofungin derivatives, Front. Microbiol. 12 (2021) 635268, doi:10.3389/fmicb.2021.635268.
[9] M.R. Estevez, M. Myronovskyi, B. Rosenkranzer, et al., Novel fredericamycin variant overproduced by a Streptomycin-resistant *Streptomyces albus* subsp. *chlorinus* strain, Mar. Drugs 18 (6) (2020) 284–295, doi:10.3390/md18060284.
[10] D. Jiang, K. Xin, B. Yang, et al., Total synthesis of three families of natural antibiotics: anthrabenzoxocinones, fasamycins/naphthacemycins, and benastatins, CCS Chem. 2 (6) (2020) 800–812, doi:10.31635/ccschem.020.202000151.
[11] M. Brasholz, S. Sörgel, C. Azap, et al., Rubromycins: structurally intriguing, biologically valuable, synthetically challenging antitumour antibiotics, Eur. J. Org. Chem. 2007 (23) (2007) 3801–3814, doi:10.1002/ejoc.200601054.
[12] D.J. Atkinson, M.A. Brimble, Isolation, biological activity, biosynthesis and synthetic studies towards the rubromycin family of natural products, Nat. Prod. Rep. 32 (6) (2015) 811–840, doi:10.1039/c4np00153b.
[13] B. Frensch, T. Lechtenberg, M. Kather, et al., Enzymatic spiroketal formation via oxidative rearrangement of pentangular polyketides, Nat. Commun. 12 (1) (2021) 1431–1442, doi:10.1038/s41467-021-21432-9.
[14] S. Wu, T. Huang, D. Xie, et al., Xantholipin B produced by the stnR inactivation mutant *Streptomyces flocculus* CGMCC 4.1223 WJN-1, J. Antibiot. 70 (1) (2017) 90–95, doi:10.1038/ja.2016.60.
[15] K.B. Herath, H. Jayasuriya, Z. Guan, et al., Anthrabenzoxocinones from *Streptomyces* sp. as liver X receptor ligands and antibacterial agents, J. Nat. Prod. 68 (9) (2005) 1437–1440, doi:10.1002/asna.200811150.
[16] Z. Qin, J.T. Munnoch, R. Devine, et al., Formicamycins, antibacterial polyketides produced by *Streptomyces formicae* isolated from African *Tetraponera* plant-ants, Chem. Sci. 8 (4) (2017) 3218–3227, doi:10.1039/c6sc04265a.
[17] T.Y. Yuen, Y.P. Ng, F. Ip, et al., Telomerase inhibition studies of novel spiroketal-containing rubromycin derivatives, Aust. J. Chem. 66 (5) (2013) 530–533, doi:10.1071/CH13035.
[18] X. Wang, S.I. Elshahawi, L.V. Ponomareva, et al., Structure determination, functional characterization, and biosynthetic implications of nybomycin metabolites from a mining reclamation site-associated *Streptomyces*, J. Nat. Prod. 82 (12) (2019) 3469–3476, doi:10.1021/acs.jnatprod.9b01015.
[19] G. Panzone, A. Trani, P. Ferrari, et al., Isolation and structure elucidation of 7,8-Dideoxy-6-oxo-griseorhodin C produced by actinoplanes ianthinogenes, J. Antibiot. 50 (8) (1997) 665–670, doi:10.7164/antibiotics.50.665.
[20] C. Puder, S. Loya, A. Hizi, et al., Structural and biosynthetic investigations of the rubromycins, Eur. J. Org. Chem. 2000 (5) (2000) 729–735, doi:10.1002/(SICI)1099-0690(200003)2000:5<729::AID-EJOC729>3.0.CO;2-2.
[21] H. Brockmann, K.H. Renneberg, Collinomycin, ein gelbes antibiotikum aus actinomyceten, Naturwissenschaften 40 (5) (1953) 166–167, doi:10.1007/BF00639946.
[22] H. Brockmann, W. Lenk, G. Schwantje, et al., Zur kenntnis der rubromycine, Tetrahedron. Lett. 7 (30) (1966) 3525–3530, doi:10.1016/S0040-4039(01)82822-7.
[23] H. Brockmann, K.H. Renneberg, Rubromycin, ein rotes antibiotikum aus actinomyceten, Naturwissenschaften 40 (2) (1953) 59–60, doi:10.1007/BF00596449.
[24] G. Bringmann, J. Kraus, U. Schmitt, et al., Determination of the absolute configurations of $\gamma$-rubromycin and related spiro compounds by Quantum chemical CD calculations, Eur. J. Org. Chem. 2000 (2000) 2729–2734, doi:10.1002/1099-0690(200008)2000:15<2729::AID-EJOC2729>3.0.CO;2-Z.
[25] L.W. Yi, J.Q. Kong, Y. Xiong, et al., Genome mining of *Streptomyces* sp. CB00271 as a natural high-producer of $\beta$-rubromycin and the resulting discovery of $\beta$-rubromycin acid, Biotechnol. Bioeng. 118 (6) (2021) 2243–2254, doi:10.1002/bit.27732.
[26] C. Coronelli, H. Pagani, M.R. Bardone, et al., Purpuromycin, a new antibiotic isolated from *Actinoplanes Ianthinogenes* N. sp, J. Antibiot. 27 (3) (1974) 161–168, doi:10.7164/antibiotics.27.161.
[27] M.R. Bardone, E. Martinelli, L.F. Zerilli, et al., Structure determination of purpuromycin, a new antibiotic, Tetrahedron 30 (1974) 2747–2754, doi:10.1016/S0040-4020(01)97439-3.
[28] S.P. Waters, M.W. Fennie, M.C. Kozlowski, Convergent route to the purpuromycin bisphenolic spiroketal: hydrogen bonding control of spiroketalization stereochemistry, Tetrahedron. Lett. 47 (30) (2006) 5409–5413, doi:10.1016/j.tetlet.2006.05.044.
[29] M. Chino, K. Nishikawa, M. Umekita, et al., Heliquinomycin, a new inhibitor of DNA helicase, produced by *Streptomyces* sp. MJ929-SF2 I. Taxonomy, production, isolation, physico-chemical properties and biological activities, J. Antibiot. 49 (1996) 752–757, doi:10.1002/chin.199706230.
[30] Chino, Nishikawa, Tsuchida, et al., Heliquinomycin, a new inhibitor of DNA helicase, produced by *Streptomyces* sp. MJ929-SF2 II. Structure determination of heliquinomycin, J. Antibiot. 50 (1997) 143–146, doi:10.7164/antibiotics.50.143.

[31] C. Su, C. Liu, Y. Wang, et al., A new heliquinomycin analogue with immunosuppressive activity from *Streptomyces* sp. jys28, Rec, Nat. Prod. 13 (6) (2019) 456–461, doi:10.25135/rnp.123.18.12.1085.
[32] X. Zhuang, Z. Wang, C. Peng, et al., Characterization of *Streptomyces piniterrae* sp. nov. and identification of the putative gene cluster encoding the biosynthesis of heliquinomycins, Microorganisms 8 (2020) 495, doi:10.3390/microorganisms8040495.
[33] E. Harunari, C. Imada, Y. Igarashi, et al., Hyaluromycin, a new hyaluronidase inhibitor of polyketide origin from marine *Streptomyces* sp, Mar. Drugs 12 (1) (2014) 491–507, doi:10.3390/md12010491.
[34] E. Harunari, C. Imada, Y. Igarashi, Konamycins A and B and rubromycins CA1 and CA2, aromatic polyketides from the tunicate-derived *Streptomyces hyaluromycini* MB-PO13(T), J. Nat. Prod. 82 (6) (2019) 1609–1615, doi:10.1021/acs.jnatprod.9b00107.
[35] W. Treibs, K. Eckardt, Über Griseorhodin A, ein neues rotes antibiotikum aus actinomyceten, Naturwissenschaften 48 (11) (1961) 430, doi:10.1007/BF00621679.
[36] K. Eckardt, D. Tresselt, W. Ihn, Antibiotika aus actinomyceten. zur chemischen konstitution des antibiotikums griseorhodin A: I—isolierung und struktur von zwei abbauprodukten, Tetrahedron 34 (4) (1978) 399–404, doi:10.1016/0040-4020(78)80022-2.
[37] D. Tresselt, K. Eckardt, W. Ihn, Antibiotika aus actinomyceten. zur chemischen konstitution des antibiotikums griseorhodin A: II. ableitung der struktur, Tetrahedron 34 (17) (1978) 2693–2699, doi:10.1016/0040-4020(78)88406-3.
[38] K. Eckardt, D. Tresselt, W. Ihn, The structure of the antibiotic griseorhodin C, J. Antibiot. 31 (1978) 970–973, doi:10.7164/antibiotics.31.970.
[39] Z. Yunt, K. Reinhardt, A. Li, et al., Cleavage of four carbon-carbon bonds during biosynthesis of the griseorhodin a spiroketal pharmacophore, J. Am. Chem. Soc. 131 (6) (2009) 2297–2305, doi:10.1021/ja807827k.
[40] H.E. Ortega, J.M. Batista, W.G.P. Melo, et al., Absolute configurations of griseorhodins A and C, Tetrahedron. Lett. 58 (50) (2017) 4721–4723, doi:10.1016/j.tetlet.2017.11.008.
[41] H.E. Ortega, J.B. Jr, W. Melo, et al., Corrigendum to "Absolute configurations of griseorhodins A and C" [Tetrahedron. Lett., 58 (50) (2017) 4721-4723], Tetrahedron. Lett. 59 (13) (2018) 1239, doi:10.1016/j.tetlet.2018.02.042.
[42] R.M. Stroshane, J.A. Chan, E.A. Rubalcaba, et al., Isolation and structure elucidation of a novel griseorhodin, J. Antibiot. 32 (3) (1979) 197–204, doi:10.7164/antibiotics.32.197.
[43] Kunio, Suetsuna, Yutaka, et al., Isolation of structure of dideoxy-griseorhodin C produced by a *Streptomyces* sp, Agric. Biol. Chem. 53 (1) (1989) 241–242, doi:10.1080/00021369.1989.10869274.
[44] J. Yang, S. Fan, H. Pei, et al., 8-Methoxygriseorhodin C, a new member of griseorhodin antibiotic, J. Antibiot. 44 (11) (1991) 1277–1279, doi:10.7164/antibiotics.44.1277.
[45] B.W. Miller, J.P. Torres, J.O. Tun, et al., Synergistic anti-methicillin-resistant *Staphylococcus aureus* (MRSA) activity and absolute stereochemistry of 7,8-dideoxygriseorhodin C, J. Antibiot. 73 (4) (2020) 290–298, doi:10.1038/s41429-019-0275-8.
[46] Y.Y. Li, X.M. Tan, J. Yang, et al., Naturally occurring seco-sativene sesquiterpenoid: chemistry and biology, J. Agric. Food. Chem. 68 (37) (2020) 9827–9838, doi:10.1021/acs.jafc.0c04560.
[47] M. Chino, K. Nishikawa, T. Tsuchida, et al., Heliquinomycin, a new inhibitor of DNA helicase, produced by *Streptomyces* sp. MJ929-SF2. III. Biosynthesis, J. Antibiot. 50 (30) (1997) 781–784, doi:10.1002/chin.199730221.
[48] R. Martin, O. Sterner, M.A. Alvarez, et al., Collinone, a new recombinant angular polyketide antibiotic made by an engineered *Streptomyces* Strain, J. Antibiot. 54 (3) (2001) 239–249, doi:10.7164/antibiotics.54.239.
[49] A. Li, J. Piel, A gene cluster from a marine *Streptomyces* encoding the biosynthesis of the aromatic spiroketal polyketide griseorhodin A, Cell. Chem. Biol. 9 (9) (2002) 1017–1026, doi:10.1016/S1074-5521(02)00223-5.
[50] M. Toplak, R. Saleem-Batcha, J. Piel, et al., Catalytic control of spiroketal formation in rubromycin polyketide biosynthesis, Angew. Chem. Int. Ed. 60 (52) (2021) 26960–26970, doi:10.1002/anie.202109384.
[51] Z.J. Lin, M.M. Zachariah, L. Marett, et al., Griseorhodins D-F, neuroactive intermediates and end products of post-PKS tailoring modification in griseorhodin biosynthesis, J. Nat. Prod. 77 (5) (2014) 1224–1230, doi:10.1021/np500155d.
[52] L.Y. Chen, J. Sperry, N.Y. Ip, et al., Natural products targeting telomere maintenance, Med. Chem. Commun. 2 (4) (2011) 229, doi:10.1039/c0md00241k.
[53] Y. Mizushina, T. Takeuchi, F. Sugawara, et al., Anti-cancer targeting telomerase inhibitors: $\beta$-rubromycin and oleic acid, Mini-Rev. Med. Chem. 12 (11) (2012) 1135–1143, doi:10.2174/138955712802762220.
[54] T. Ueno, H. Takahashi, M. Oda, et al., Inhibition of human telomerase by rubromycins: implication of spiroketal system of the compounds as an active moiety, Biochemistry 39 (20) (2000) 5995–6002, doi:10.1021/bi992661i.
[55] M.E. Goldman, G.S. Salituro, J.A. Bowen, et al., Inhibition of human immunodeficiency virus-1 reverse transcriptase activity by rubromycins: competitive interaction at the template.primer site, Mol. Pharmacol. 38 (1) (1990) 20–25, doi:10.1002/med.2610100304.
[56] Y. Mizushina, T. Ueno, M. Oda, et al., The biochemical mode of inhibition of DNA polymerase $\beta$ by $\alpha$-rubromycin, BBA-Gen. Subj. 1523 (2) (2000) 172–181, doi:10.1016/S0304-4165(00)00119-7.
[57] H.A. Alhadrami, A.M. Sayed, H. Al-Khatabi, et al., Scaffold hopping of $\alpha$-rubromycin enables direct access to FDA-approved cromoglicic acid as a SARS-CoV-2 $M^{Pro}$ inhibitor, Pharmaceuticals 14 (6) (2021) 541, doi:10.3390/ph14060541.
[58] S. Tani, N. Nishio, K. Kai, et al., Chemical genetic approach using $\beta$-rubromycin reveals that a RIO kinase-like protein is involved in morphological development in phytophthora infestans, Sci. Rep. 10 (1) (2020) 22326, doi:10.1038/s41598-020-79326-7.
[59] B.A.P. Wilson, C.C. Thornburg, C.J. Henrich, et al., Creating and screening natural product libraries, Nat. Prod. Rep. 37 (7) (2020) 893–918, doi:10.1039/C9NP00068B.
[60] J.L. Wolfender, M. Litaudon, D. Touboul, et al., Innovative omics-based approaches for prioritisation and targeted isolation of natural products – new strategies for drug discovery, Nat. Prod. Rep. 36 (6) (2019) 855–868, doi:10.1039/C9NP00004F.
[61] A.E.F. Ramos, L. Evanno, E. Poupon, et al., Natural products targeting strategies involving molecular networking: different manners, one goal, Nat. Prod. Rep. 36 (7) (2019) 960–980, doi:10.1039/C9NP00006B.